Doubly-Fed Induction Generator Drive System Based on Maximum Power Curve Searching using Fuzzy Logic Controller

Abdelhak Dida*, Djilani Benattous**
* Department of Electrical Engineering, Biskra University, Biskra, 07000, Algeria
** Department of Electrical Engineering, El-Oued University, El Oued 39000, Algeria

Article Info

Article history:

Received Dec 18, 2014
Revised Feb 7, 2015
Accepted Feb 25, 2015

Keyword:

DFIG
Fuzzy logic controller
Maximum power point tracking
Maximum power curve
Wind turbine

ABSTRACT

This paper proposes a novel variable speed control algorithm for a grid connected doubly-fed induction generator (DFIG) system. The main objective is to track the maximum power curve characteristic by using an adaptive fuzzy logic controller, and to compare it with the conventional optimal torque control method for large inertia wind turbines. The role of the FLC is to adapt the transfer function of the harvested mechanical power controller according to the operating point in variable wind speed. The control system has two sub-systems for the rotor side and the grid side converters (RSC, GSC). Active and reactive power control of the back-to-back converters has been achieved indirectly by controlling q-axis and d-axis current components. The main function of the RSC controllers is to track the maximum power through controlling the electromagnetic torque of the wind turbine. The GSC controls the DC-link voltage, and guarantees unity power factor between the GSC and the grid. The proposed system is developed and tested in MATLAB/SimPowerSystem (SPS) environment.

Corresponding Author:

Abdelhak Dida,
Department of Electrical Engineering,
Biskra University,
Biskra, 07000, Algeria.
Email: abdelhakdida@yahoo.fr

1. INTRODUCTION

Doubly-fed induction generators (DFIGs) have been widely used for large scale wind generation systems, and their control and operations have been the subject of intense research during the last few years. The response and performance of DFIG based wind turbines during steady state and transient conditions under symmetrical stator voltage supply are now well understood [1]-[2]. Wind turbines are controlled to operate only in a specified range of wind speeds bounded by cut-in and cut-out speeds. Beyond these limits, the turbine should be stopped to protect both the generator and turbine. Fig. 1 shows the typical power curve of a wind turbine [3]-[4].

In order to get the optimal operating point of the wind turbine, including a maximum power point tracking (MPPT) algorithm in the system is essential [5]. Much has been written on the topic of MPPT algorithms, namely, tip speed ratio (TSR) control [6-7], optimal torque (OT) control [5], robust control [6]-[8], power signal feedback (PSF) control [9]-[10] and hill-climb searching (HCS) control [11]-[5]. TSR control regulates the wind turbine rotor speed to maintain an optimal TSR at which maximum power is extracted [7], this technique is limited by the difficulty to obtain the optimal TSR and the wind speed measurement [6]-[12]. PSF control requires the knowledge of the wind turbine's maximum power curve (MPC), and tracks this curve through its control mechanisms. According to [8]-[9], it's difficult to obtain with accuracy the MPC in practical applications. The HCS technique does not require wind speed data or the turbine characteristics [13].

The MPC can be used as mechanical power reference needs to be tracked by the harvested mechanical power of the rotating shaft. The OT control is distinguished by its fast response and its high efficiency, thus we choose the electromagnetic torque as output of the proposed MPPT algorithm, and this can improve the rapidity of the convergence speed. Under powerful wind turbulence, a typical proportional-integral (PI) controller may be not the right choice, but an intelligent FLC can do the job with its adaptive reasoning capability. The FLC is nonlinear controller easy to implement, and the key behind its good performance is by adjusting the scaling factors and the membership function shape which are not hard task for someone who is an expert.

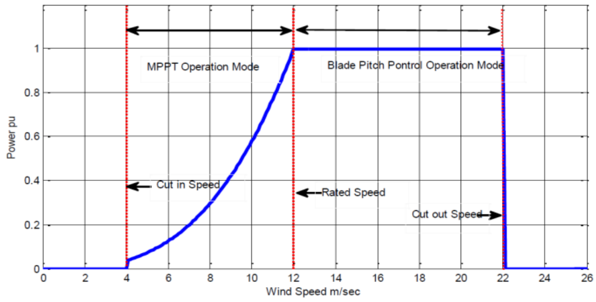

Figure 1. Power curve of a variable speed wind turbine

In this study, a maximum power curve searching (MPCS) approach based on fuzzy logic is adopted as MPPT algorithm, and compared to another MPPT approach with good performance like the OT control method, and to achieve an intelligent control of electromagnetic torque. Simulation investigations have been conducted on a 1.5MW DFIG to verify the researched study.

2. VECTOR CONTROL OF THE DFIG

We choose a d-q representation of the DFIG, with the *d*-axis oriented along the stator-flux vector position. Since the stator is connected to the grid, we could make the following assumptions [14]:

a) The stator resistance R_s can be *neglected* (usually justified in machines with a rating over 10kW).

b) The stator magnetizing current space phasor $\vec{i}_{ms}$ is constant in magnitude and phase.

c) Frequency of the power supply on the stator is constant, i.e. $\omega_s = constant$

Under those assumptions, it implies that:

$$\begin{cases} \Phi_{sd} = \Phi_s = L_m \left| \vec{i}_{ms} \right| = \dfrac{\left| \vec{V}_s \right|}{\omega_s} \\ \Phi_{sq} = L_s i_{sq} + L_m i_{rq} = 0 \\ \Phi_{rd} = \dfrac{L_m^2}{L_s} \left| \vec{i}_{ms} \right| + \sigma L_r i_{rd} \\ \Phi_{rq} = \sigma L_r i_{rq} \end{cases} \qquad (1)$$

Where $\sigma = 1 - L_m^2 / L_s L_r$ and $\left| \vec{V}_s \right| = \sqrt{3} V_s$, V_s is the RMS of the stator-voltage space phasor in the stationary reference frame $\vec{V}_s = \sqrt{3} V_s e^{jw_s t}$. The stator and rotor voltage can be written as [14]:

$$\begin{cases} V_{sd} = R_s i_{sd} + \dfrac{d\Phi_{sd}}{dt} - \omega_s \Phi_{sq} \approx 0 \\ V_{sq} = R_s i_{sq} + \dfrac{d\Phi_{sq}}{dt} + \omega_s \Phi_{sd} \approx \omega_s \Phi_{sd} = \left|\vec{V}_s\right| \\ V_{rd} = R_r i_{rd} + \sigma L_r \dfrac{di_{rd}}{dt} - (\omega_s - \omega_e)\sigma L_r i_{rq} \\ V_{rq} = R_r i_{rq} + \sigma L_r \dfrac{di_{rq}}{dt} - (\omega_s - \omega_e)(\dfrac{L_m^2}{L_s}\left|\vec{i}_{ms}\right| + \sigma L_r i_{rd}) \end{cases} \tag{2}$$

Where ω_s and $\omega_e = p\omega_m$ are the synchronous and the generator speed respectively. We define in Equation (3) the $V_{rd}^{'}$ and $V_{rq}^{'}$ as the outputs of the PI current controllers. Voltages V_{rd} and V_{rd} will be used to control the rotor voltages through the RSC.

$$\begin{cases} V_{rd}^{'} = R_r i_{rd} + \sigma L_r \dfrac{di_{rd}}{dt} \\ V_{rq}^{'} = R_r i_{rq} + \sigma L_r \dfrac{di_{rq}}{dt} \end{cases} \tag{3}$$

We rewrite the stator active and reactive power, and the electromagnetic torque equations as:

$$\begin{cases} T_{em} = -p \dfrac{L_m^2}{L_s}\left|\vec{i}_{ms}\right| i_{rq} \\ Q_s = -\left|\vec{V}_s\right| \dfrac{L_m}{L_s} i_{rd} + \left|\vec{V}_s\right|^2 \dfrac{1}{\omega_s L_s} \end{cases} \tag{4}$$

From Equation (4), it can be seen that the electromagnetic torque depends only on the q-axis rotor current. The stator reactive power only depends on the d-axis rotor current. Therefore, the indirect vector control of stator active and reactive power has been achieved in the stator-flux reference frame and presented in Figure 2. PI control is typically used for the rotor currents loops and can satisfy the control requirement under normal operation conditions.

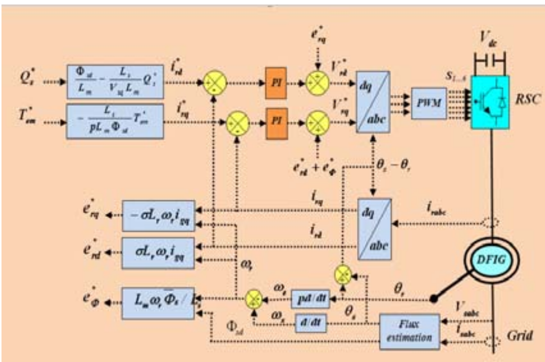

Figure 2. Vector control of the DFIG

3. VECTOR CONTROL OF GSC

The control objective of the GSC is to maintain constant DC-link voltage regardless of the changing rotor power. Vector control has been applied to enable decoupled control of the active and reactive powers flowing between the grid and the GSC through the choke [15]. The voltage equations in the d-q frame rotating at grid voltage pulsation are given as follows:

$$\begin{cases} V_{fd} = R_g i_{gd} + L \dfrac{di_{gd}}{dt} - \omega_s L_g i_{gq} + V_{gd} \\ V_{fq} = R_g i_{gq} + L \dfrac{di_{gq}}{dt} + \omega_s L_g i_{gd} + V_{gq} \end{cases} \tag{5}$$

The rotating reference frame is aligned with the grid voltage, so we obtain:

$$V_{gd} = \sqrt{3} V_g = \left| \vec{V}_g \right| \qquad and \qquad V_{gq} = 0 \tag{6}$$

The angle position of the grid voltage is computed as:

$$\theta_s = \int \omega_s dt = \tan^{-1} \frac{V_{s\beta}}{V_{s\alpha}} \tag{7}$$

Thus we can write the active and reactive power equations of the GSC as:

$$\begin{cases} P_g = \left| \vec{V}_g \right| i_{gd} \\ Q_g = - \left| \vec{V}_g \right| i_{gq} \end{cases} \tag{8}$$

It can be clearly seen that active and reactive powers are proportional to i_{gd} and i_{gq} respectively. Therefore we can achieve the decoupled control of the active and reactive powers through i_{gd} and i_{gq}. We assume the back-to-back converter is lossless and neglect the losses in the inductor resistance (choke), we also assume that harmonics due to the switching can be neglected, then based on the DC-link model we have:

$$i_{c-dc} = C_{dc} \frac{dV_{dc}}{dt} = i_{g-dc} - i_{r-dc} \tag{9}$$

$$\begin{cases} P_g = V_{dc} i_{g-dc} = \left| \vec{V}_g \right| i_{gd} \\ \left| \vec{V}_g \right| = \dfrac{m_{GSC}}{2} V_{dc} \\ i_{g-dc} = \dfrac{m_{GSC}}{2} i_{gd} \end{cases} \tag{10}$$

Where m_{GSC} is the modulation index of the GSC. We consider i_{r-dc} as distance, and apply Laplace transform to Equation (9) then we can obtain the V_{dc} as function of i_{gd}:

$$V_{dc} = \frac{m_{GSC}}{2 C_{dc} . s} i_{gd}(s) \tag{11}$$

Where s is the Laplace operator.

A PI controller has been used to guarantee constant DC-link voltage and generate reference *d*-axis current component i_{gd}^* to the inner control loop. We set $i_{gq}^* = 0$ because we want the grid-side reactive power to be zero. We define $V_{GSC-d}^{'}$ and $V_{GSC-q}^{'}$ as the outputs of the inner PI current controllers, then from voltage Equation (5), the reference converter voltages are:

$$\begin{cases} V_{fd}^* = V_{fd}^{'} + (\omega_s L_g i_{gq} + V_{gd}) \\ V_{fq}^* = V_{fq}^{'} - \omega_s L_g i_{gd} \end{cases} \tag{12}$$

The overall control structure of the GSC is presented in Figure 3.

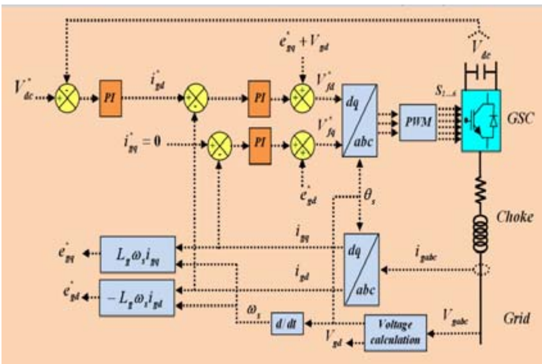

Figure 3. Vector control of the GSC

4. WIND TURBINE MODELING AND CONTROL

4.1. Wind Turbine Model

The turbine is the prime mover of WECS that enables the conversion of kinetic energy of wind E_w into mechanical power P_m and eventually into electrical energy [16].

$$\begin{cases} P_m = \dfrac{\partial E_w}{\partial t} C_p = \dfrac{1}{2}\rho A V_w^3 C_p(\lambda, \beta) \\ C_p(\lambda, \beta) = 0.22\left(\dfrac{116}{\lambda_i} - 0.4\beta - 5\right) e^{\frac{-12.5}{\lambda_i}} \end{cases} \tag{13}$$

Where V_w is the wind speed at the center of the rotor (m/s), ρ is the air density (Kg/m^3), $A=\pi R^2$ is the frontal area of the wind turbine (m^2) and R is the rotor radius (m). C_p is the efficiency coefficient which in turn depends upon the turbine characteristics (β - blade pitch angle, and λ- TSR) that is responsible for the losses in the energy conversion process, and $\lambda_i = f(\lambda, \beta)$ is given by:

$$\begin{cases} \lambda = \dfrac{\omega_t R}{V_w} \\ \dfrac{1}{\lambda_i} = \dfrac{1}{\lambda + 0.08\beta} - \dfrac{0.035}{\beta^3 + 1} \end{cases} \tag{14}$$

3.2. Two-mass Drive Traine Model

The power transmission from turbine axis to generator axis is done by a component called drive-train. Three different drive-train models (one, two, and three-mass models) usually used to model the drive-train [17]. The so-called two-mass model is simple and sufficient with reasonable accuracy, for the transient stability analysis especially the interaction with the grid [18]-[19], the two-mass drive-train structure is shown in Figure 4.

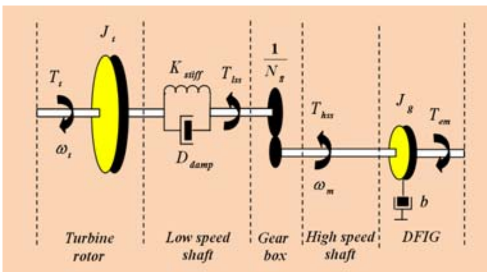

Figure 4. Two-mass drive train model

The aerodynamic torque T_t causes the turbine speed ω_m, which gives the dynamic equations as follows [20]:

$$J_t \frac{d\omega_t}{dt} = T_t - T_{lss} \tag{15}$$

Here, the low-speed shaft torque T_{lss} acts as a braking torque, it is obtained by Equation (16):

$$\begin{cases} T_{lss} = K_{stiff}(\theta_t - \frac{\theta_m}{N_g}) + D_{damp}(\omega_t - \frac{\omega_m}{N_g}) = N_g T_{hss} \\ \dot{\theta}_t = \omega_t \, and \, \dot{\theta}_m = \omega_m \end{cases} \tag{16}$$

The generator inertia J_g is driven through the high-speed shaft, the high-speed shaft torque T_{hss} is braked by generator electromagnetic torque T_{em}, its dynamic system is described by:

$$J_g \frac{d\omega_m}{dt} = T_{hss} - T_{em} - b\,\omega_m \tag{17}$$

Where: T_t and T_g: aerodynamic torque of turbine rotor and generator electromagnetic torque respectively,
J_t and J_g: : turbine rotor and generator moment of inertia respectively,
ω_t and ω_m : turbine rotor and generator mechanical speed respectively,

5. MAXIMUM POWER CURVE SEARCHING ALGORITHM

The maximum power curve searching (MPCS) method is one of numerous solutions for maximizing the output power in wind turbine system, it is based on the MPC characteristic which depends of the structural characteristics of the wind turbine which somehow similar to the OT control, another similarity is the output electromagnetic torque of reference which enforce the rapidness of the proposed algorithm. After the estimation of MPC characteristic, and the harvested mechanical power in the rotating shaft with considering all the electrical and mechanical losses (∑losses) in the wind turbine. A fuzzy logic controller with its adaptive reasoning is applied to unsure the convergence of the proposed method through variable output step-size signal until the error becomes zero. If the operating point is to the left of the peak point after changing in the wind speed (point A), the controller must move it to the right to be closer to the peak until it gets to the zero error (point B), and vice versa if it is on the other side as shown in Figure 5. Additionally, choosing an appropriate step-size (or scaling factors) in the output is not an easy task, though larger step-size means a faster response and more oscillations around the peak point, and hence, less efficiency, a smaller step-size may threat the convergence of the system.

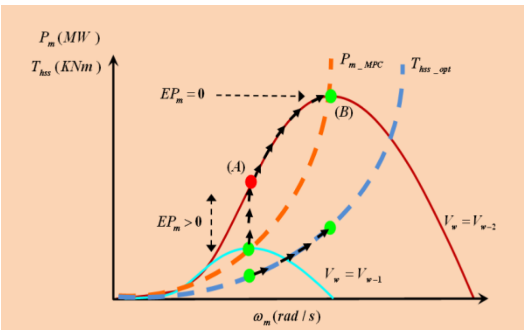

Figure 5. Working mechanism of MPCS approach

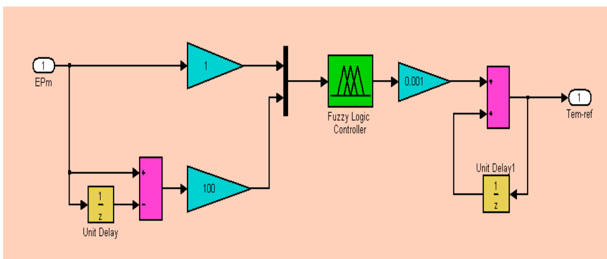

Figure 6. FLC structure of the mechanical power

Fuzzy logic control has the capability to control nonlinear, uncertain and adaptive systems, which gives strong robust performance for parameter variation [21]-[22]. The general structure of a fuzzy like-PI controller is shown in Figure 6 where the input signals are the error and its change (E and ΔE) and the output signal is the command change (ΔU). The fuzzy Membership functions (MFs) are defined as follows:

Z=zero, *PS*=Positive Small, *PM*=Positive Medium, *PB*=Positive Big, *NS*=Negative small, *NM*= Negative Medium, *NB*= Negative Big.

FLC rules table consists of series "*if-and-then*" fuzzy logic condition sentences. The design of these rules is based on a qualitative knowledge, deduced from extensive simulation tests using a conventional PI controller of the system for different values of K_p and K_i, and with different operating conditions [23].

In this study, the measured rotational speed and stator power will be used as inputs to the MPPT system, the error in estimated mechanical power and its change (EP_m and ΔEP_m) are used as inputs to the FLC, and the output is the change on electromagnetic torque of reference (ΔT_{em}^*). MFs and the surface created by the fuzzy controller are shown in Figure 7. Triangular symmetrical membership functions are suitable for the input and output, which give more sensitivity especially as variables approach to zero. Table 1 gives the corresponding rule of this Fuzzy-MPCS controller. The FLC is efficient to track the maximum power point, especially in case of frequently changing wind conditions [24]. The overall block diagram of the MPPT control is shown in Figure 8. By estimating all the electrical and mechanical losses in the wind turbine, the following relations are obtained:

$$P_m = P_s + P_r + \sum losses = (1-g)P_s + 0.1 * P_m \tag{18}$$

$$P_m = (1-g)P_s * 1.1111 \tag{19}$$

For defining the MPC and according to the Equation (13) and (14), if the rotor is running at the optimal TSR (λ_{opt}), it will also run at C_{pmax}. Thus, the MPC expression is obtained:

$$P_{m\_MPC} = \frac{1}{2}\rho\pi R^5 \frac{C_{p\max}}{\lambda_{opt}^3}\omega_m^3 = K_{opt}\,\omega_m^3 \tag{20}$$

This MPC relation is used as reference to the mechanical power loop.

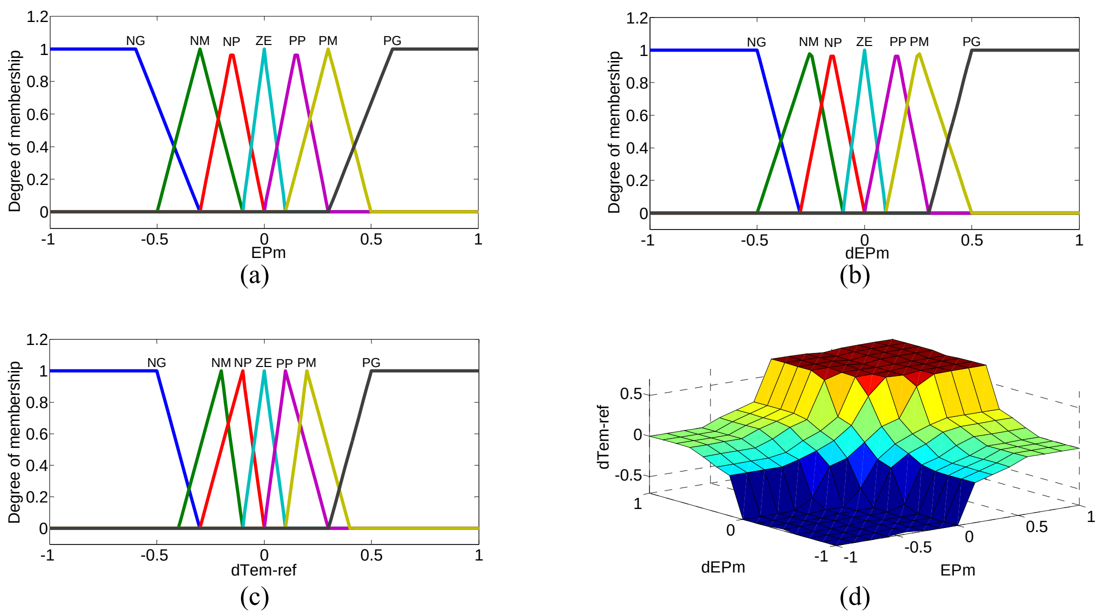

Figure 7. Membership functions of Fuzzy-MPCS controller
(a,b) Input membership functions of EP_m and ΔEP_m respectively (c) Output membership functions of $\Delta T_{em\text{-}ref}$
(d) Surface created by the fuzzy controller

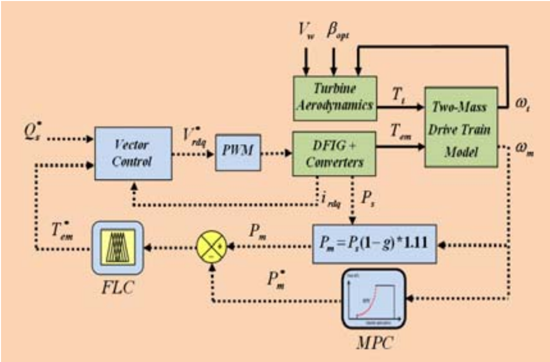

Figure 8. Block diagram of MPCS-MPPT control system

Table 1. Rule table of Fuzzy-MPCS controller

EP_m(pu) / ΔEP_m(pu)	NB	NM	NS	Z	PS	PM	PB
NB	NB	NB	NB	NB	NM	NS	Z
NM	NB	NB	NB	NM	NS	Z	PS
NS	NB	NB	NM	NS	Z	PS	PM
Z	NB	NM	NS	Z	PS	PM	PB
PS	NM	NS	Z	PS	PM	PB	PB
PM	NS	Z	PS	PM	PB	PB	PB
PB	Z	PS	PM	PB	PB	PB	PB

In order to be honest, we have to compare the MPCS algorithm with a good sensorless MPPT method, the OT control seems suitable with its superiority in term of efficiency and speed of response, However, the efficiency is lower compared to that of TSR control method, because it does not use the wind speed directly, meaning that wind changes are not reflected instantaneously and significantly on the reference signal [25]. Considering that $P_m=T_{hss}\omega_m$ in the high speed shaft and with considering Equation (20), T_{hss} can be rearranged as follows:

$$T_{hss\_opt} = \frac{1}{2}\rho\pi R^5 \frac{C_{p\max}}{\lambda_{opt}^3}\omega_m^2 = K_{opt}\,\omega_m^2 \tag{21}$$

The OT is a torque control based method, where the analytical expression of the optimum torque curve, represented by Equation (21), is given as a reference torque for the controller that is connected to the wind turbine [5]. The overall diagram of the OT control is represented in Figure 9. According to the wind turbine parameters mentioned in the appendix, the 1.5MW wind turbine characteristics are shown in Figure 10, this yield to K_{opt} = 0.436

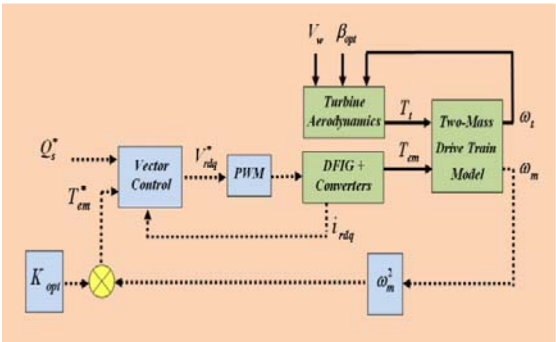

Figure 9. Block diagram of OT control MPPT method

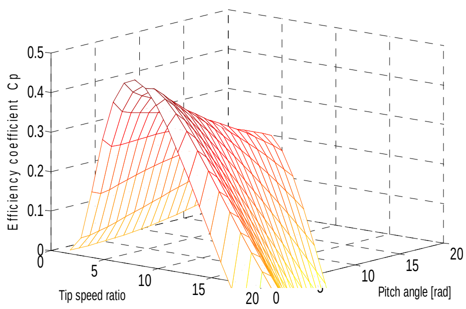

Figure 10. Power coefficient curve versus TSR and pitch angle

6. SIMULATION RESULTS AND DISCUSSION

Investigation has been performed on a 1.5MW DFIG system incorporating the proposed Fuzzy-MPCS controller. The parameters of the DFIG are inspired from [14]-[26]. The simulation objective is to apply a random wind speed profile to emulate normal wind turbulence; the proposed MPCS strategy has to give the optimal electromagnetic torque to the system, and to contend the OT control method in terms of efficiency and speed of response. The wind speed profile is chosen in order to cover the whole variable speed operating mode of the DFIG system which is between the 1.2 and 0.7 [pu]. The control system is performed in the per-unit (pu) system according to the rated characteristics of the wind turbine (see appendix), the simulation results are denoted in Figure 11.

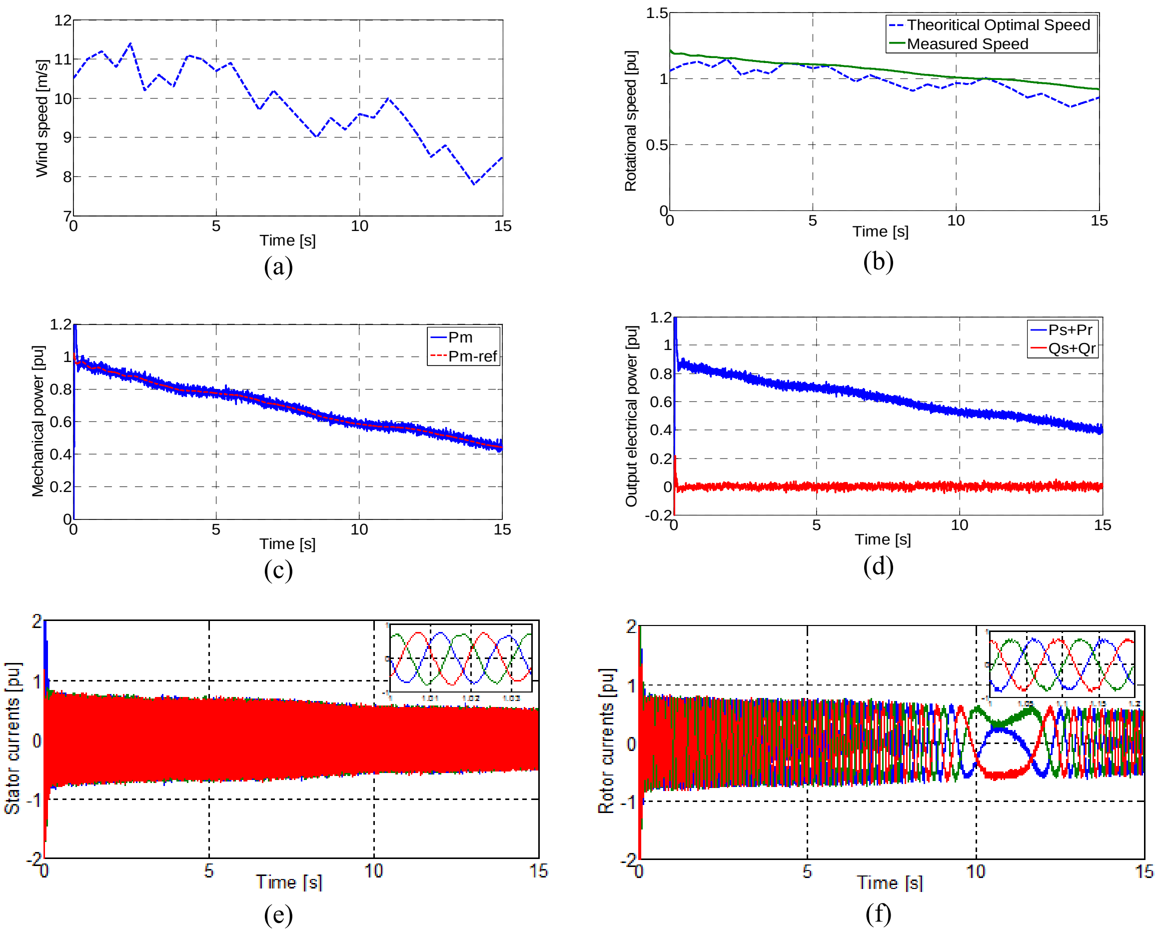

Figure 11. Dynamic responses of the fuzzy-MPCS algorithm in the variable speed mode
(a) Wind speed profile (b) Rotational speed (c) Mechanical power (d) Output electrical power
(e) Stator currents (f) Rotor currents

The Figure 11 shows the dynamic response of the wind turbine, the Figure 11(a) shows a random wind speed profile covered almost the whole variable speed operating range of wind speed, bounded by cut-in and the rated wind speeds. The Figure 11(b) shows the rotational speed response and its theoretical optimal value, it is changing according to the wind speed value, and compared with the OT control, the Figure 12(d) shows a good and stable response for both techniques. The Figure 11(c) shows the output mechanical power and its theoretical optimum reference according to the available kinetic power of the wind, the output mechanical power track its reference precisely thanks of the FLC. The Figure 11(d) shows the total electrical output power of the DFIG, the active power is the harvested power from the available mechanical power in the high speed shaft, it's a little bit lesser than the mechanical power because of the collective losses of the system. The Figure 11(e) and the Figure 11(f) show the stator and the rotor currents respectively obtained by the Fuzzy-MPCS control method, they are changing according to the output power magnitude, the rotor currents frequency is changing according to the rotational speed, on contrary the stator currents frequency is maintained the grid frequency.

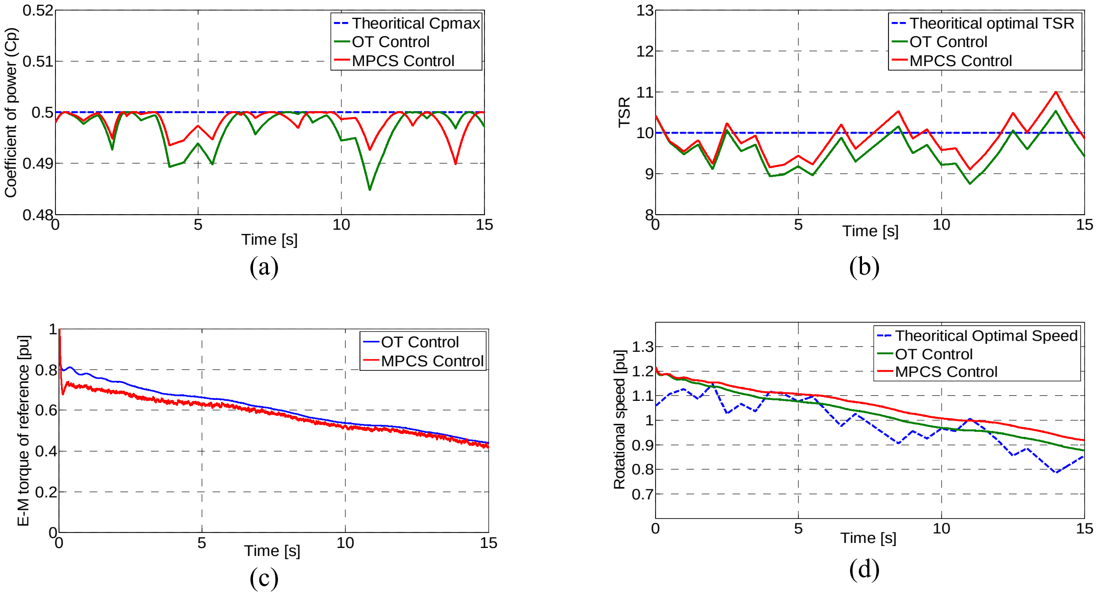

Figure 12. Dynamic response comparison between OT and MPCS control techniques
(a) Coefficient of power (b) TSR (c) Electromagnetic torque of reference (d) Rotational speed

The power coefficient response is presented in Figure 12(a), in term of speed and efficiency, the two methods seem fast and efficient, but the Fuzzy-MPCS method is a little bit superior. The Figure 12(b) shows the TSR characteristics, it reaches the optimal value and keeps it in both MPPT methods.

Table 2. Rule table of Fuzzy-MPCS controller

Technique	Principal	Complexity	Convergence speed	Wind speed measurement	Performance	Median Cp
OT Control	OT characteristics	Simple	Fast	No	Very good	0.490
MPCS Control	MPC characteristics	Simple	Fast	No	Very good	0.495

Table 3. Detailed parameters of DFIG and the wind turbine system [14]-[26]

parametre	symbole	value
Rated wind speed	V_w	12 m/s
Rated apparent power	S_{out}	1,5/0.9 MVA
Rated active power	P_{out}	1,5 MW
Rated voltage (line to line)	V_s	575 V
Rated DC-link voltage	V_{dc}	1200 V
Rated Grid frequency	f	60 Hz
Number of pole pairs	p	3
Stator/rotor turns ratio	m	1/3
Stator resistance	R_s	0.023 pu
Rotor resistance	R_r	0.016 pu
Stator leakage inductance	L_s	0.18 pu
Rotor leakage inductance	L_r	0.16 pu
Magnetizing inductance	L_m	2.9 pu
DC-link capacitance	C_{dc}	0.01 F
Choke (resistance/ inductance)	R_g /L_g	0.003 / 0.3 pu
Filter (resistance/ capacitor)	R_f / C_f	0.53 Ω / 1333 mF
Network	$V_l/l_l/Z_L$	25KV / 30Km/ (3.45+11.87)Ω
Transformer (power, voltage)	P_t, V_1/V_2	1.75 KW / (25/0.575) KV
(winding1/winding2)	(R_1/L_1) / (R_2/L_2)	(0.025/30, 0.025)pu/(0.025/30, 0.025)pu
Generator lumped inertia constant = $J_g/2$	H_g	0.685 s
Turbine lumped inertia constant = $J_t/2$	H_t	3 s
Equivalent torsional stiffness coefficient	K_{stiff}	1.11 pu
Equivalent damping coefficient	D_{damp}	1.5 pu
Generator friction coefficient	b	0.01 pu
Gearbox ratio	N_g	91
Rotor diameter	$2R$	72 m
Air density	ρ	1.225 kg/m^3

The Figure 12(c) shows optimum electromagnetic torque of reference for both the MPPT methods, they are decreased from the rated value which is 0.83[pu] into 0.4[pu] according to the wind speed and the control algorithms. The Table 2 gives a brief comparison between the two MPPT techniques in different levels. Based on results and analysis, the MPCS method was found to be fast, efficient and steady, and it's a little bit more efficient compared to the OT control because it's deal directly with the MPC characteristic of the wind turbine, and with no need to any information about the wind speed.

Table 4. Detailed parameters of the DFIG control system:

parameter	symbole	value
Power system sampling period	T_{s_power}	5e-5 s
Control system sampling period	$T_{s\_control}$	5e-5 s
Switching frequency	f_{sw}	1700 Hz
PI rotor currents controllers	$(K_{p\text{-}ir}, K_{i\text{-}ir})$	(0.3,8)
PI DC-link voltage controllers	$(K_{p\text{-}Vdc}, K_{i\text{-}Vdc})$	(8,400)
PI GSC currents controllers	$(K_{p\text{-}ig}, K_{i\text{-}ig})$	(2.5, 500)

7. CONCLUSION

This paper reviewed and discussed a novel mppt algorithm for wind turbine system equipped with dfig. In addition, the authors analyzed a simulation and comparison of the proposed algorithm with the conventional sensorless ot control method in terms of efficiency and speed of response. Simulation results demonstrated the simplicity and accuracy of the mpcs method. This method obtained the maximum average value of power coefficient and maintained it at its maximum like in the ot control method even with changes in wind speed. Nevertheless, its dependency on wind turbine characteristics made it inflexible. On the other hand, the flc is fast, flexible and simple in implementation, and can be difficult in determining the flc scaling factors which can causes more fluctuation or unstable response.

REFERENCES

[1] S Muller, M Deicke, RW De Doncker. Doubly fed induction generator systems for wind turbines. *IEEE Industry Application Magazine*. 2002; 3(1): 26–33.

[2] J Lýýpez, P Sanchis, X Roboam, L Marroyo. Dynamic behavior of the doubly fed induction generator during three-phase voltage dips. *IEEE Transactions on Energy Conversion*. 2007; 22(3): 709–717.

[3] F Bianchi, H De Battista, R Mantz. Wind turbine control systems: principles, modelling and gain-scheduling design advances in industrial control. *Lavoisier*. 2006.

[4] X Feng, Z Jianzhong, C Ming. Analysis of double objectives control for wind power generation system with frequency separation. *Fourth International Conference on Electric Utility Deregulation and Restructuring and Power Technologies (DRPT)*. 2011; 1366–1371.

[5] MA Abdullah, AHM Yatim, CW Tan, R Saidur. A review of maximum power point tracking algorithms for wind energy system. *Renewable and Sustainable Energy Reviews*. 2012; 16: 3220– 3227.

[6] T Thiringer, J Linders. Control by variable rotor speed of a fixed-pitch wind turbine operating in a wide speed range. *IEEE Transactions on Energy Conversion*. 1993; 8(3): 520–526.

[7] H Li, KL Shi, PG McLaren. Neural-network-based sensorless maximum wind energy capture with compensated power coefficient. *IEEE Transactions on Industry Applications*. 2005; 41(6): 1548–1556.

[8] MA Abdullah, AHM Yatim, C Wei Tan. A study of maximum power point tracking algorithms for wind energy system. *First IEEE Conference on Clean Energy and Technology*. 2011; 321–326.

[9] R Chedid, F Mrad, M Basma. Intelligent control of a class of wind energy conversion systems. *IEEE Transactions on Energy Conversion*. 1999; 14: 1597–1604.

[10] AB Raju, BG Fernandes, K Chatterjee. A UPF power conditioner with maximum power point tracker for grid connected variable speed wind energy conversion system. *First International Conference on PESA, Bombay, India*. 2004; 107–112.

[11] Q Wang, L Chang. An intelligent maximum power extraction algorithm for inverter-based variable speed wind turbine systems. *IEEE Transactions on Power Electronics*. 2004; 19(5): 1242–1249.

[12] E Koutroulis, K Kalaitzakis. Design of a maximum power tracking system for wind-energy-conversion applications. *IEEE Transactions Industrial Electronics*. 2006; 53(2): 486-494.

[13] AM Eltamaly, HM Farh. Maximum power extraction from wind energy system based on fuzzy logic control. *Electric Power Systems Research*. 2013; 97; 144–150.

[14] R Fadaeinedjad, M Moallem, G Moschopoulos. Simulation of a wind turbine with doubly fed induction generator by FAST and Simulink. *IEEE Transactions on energy conversion*. 2008; 23(2): 690–700.

[15] R Pena, JC Clare, GM Asher. Doubly-fed induction generator using back-to-back PWM converters and its application to variable-speed wind-energy generation. *IEE Proceeding on Electric Power Application*. 1996; 143(3): 231–241.

[16] JG Slootweg, SWH de Haan, H Polinder, WL Kling. General model for representing variable speed wind turbines in power system dynamic simulation. *IEEE Transactions on Power Systems*. 2003; 18(1): 144–151.
[17] F Iof, AD Hansen, P Sorensen, F Blaabjerg. Wind turbine blockset in MATLAB/ simulink, General overview and description of the model. Aalborg University. 2004.
[18] V Akhmatov. Modelling of Variable-Speed Wind Turbines with Doubly-Fed Induction Generators in Short Term Stability Investigations. *International Workshop on Transmission Networks for Offshore Wind Farms, Stockholm, Sweden*. 2002; 23.
[19] P Ledesma, J Usaola. Doubly Fed Induction Generator Model for Transient Stability Analysis. *IEEE Transactions on Energy Conversion*. 20(2): 388–397.
[20] B Boukhezzar, H Siguerdidjane. Nonlinear control of a variable wind turbine using a two mass model," *IEEE Transactions on Energy Conversion*. 2011; 26(1): 149–162.
[21] Y Ren, H Li, J Zhou, Z An, J Liu, H Hu, H Liu. Dynamic performance analysis of grid-connected DFIG based on fuzzy logic control. *IEEE International Conference on Mechatronics and Automation, Changchun, China*. 2009; 719-723.
[22] Y Zhao, XD Zou, YN Xu, Y Kang, J Chen. Maximal power point tracking under speed-mode control for wind energy generation system with doubly fed introduction generator. *Fifth International Power Electronics and Motion Control Conference (IPEMC 2006), Shanghai*. 2006; 1-5.
[23] C Narayan, HM Jabr. *Anovel PI gain scheduler for a vector controlled doubly-Fed wind driven induction generator*. Eighth IEEE International Conference. 2010; 2: 948-953.
[24] AG Abo-Khalil, DC Lee, JK Seok. Variable speed wind power generation system based on fuzzy logic control for maximum power output tracking. *Thirty-fifth Annual IEEE Power Electronics Specialists Conference, PESC, Aachen, Germany*. 2004; 3: 2039–2043.
[25] SM Raza Kazmi, H Goto, G Hai-Jiao, O Ichinokura. Review and critical analysis of the research papers published till date on maximum power point tracking in wind energy conversion system. *IEEE Energy Conversion Congress and Exposition (ECCE)*. 2010; 4075–82.
[26] Y Zou, M Elbuluk, Y Sozer. A complete modeling and simulation of induction generator wind power systems. *IEEE Industry Applications Society Annual Meeting (IAS)*. 2010; 1–8.

BIOGRAPHIES OF AUTHORS

Abdelhak Dida received his Engineering degree in electrical engineering from Biskra University, Algeria in 2004. He got his M. Sc degree in electric machine and its drive from Ferhat Abbas, Setif-1 University, Algeria in 2008. Now he is Doctorate candidate in department of electrical engineering at University of Biskra. He is currently assistant professor at Ferhat Abbas, Setif-1 University Algeria. His research interests include control and automation, especially the control of electrical machines, power electronics, and artificial intelligence.
E-mail: abdelhakdida@yahoo.fr (Corresponding author)

Djilani Benattous received his engineering degree in electrical engineering from Polytechnic National Institute Algiers, Algeria in 1984. He got M.Sc degree in Power Systems from UMIST England in 1987. In 2000, he received his PhD from Batna University Algeria). He is currently a professor at El-Oued University Algeria. His research interests in Planning and Economic of Electric Energy System, Optimization Theory and its applications, control of electrical machines, power electronics, and artificial intelligence. He is member of the VTRS research Laboratory.
E-mail: dbenattous@yahoo.com